NUKLEONIKA 2017;62(1):47–59
doi: 10.1515/nuka-2017-0007

ORIGINAL PAPER

Precise determination of HPGe detector efficiency for gamma spectrometry measurements of environmental samples with variable geometry and density

Manuel Barrera, Melquiades Casas-Ruiz, José J. Alonso, Juan Vidal

Abstract. A methodology to determine the full energy peak efficiency (FEPE) for precise gamma spectrometry measurements of environmental samples with high-purity germanium (HPGe) detector, valid when this efficiency depends on the energy of the radiation E, the height of the cylindrical sample H, and its density ρ, is introduced. The methodology consists of an initial calibration as a function of E and H and the application of a self-attenuation factor, depending on the density of the sample ρ, in order to correct for the different attenuation of the generic sample in relation to the measured standard. The obtained efficiency can be used in the whole range of interest studied, E = 120–2000 keV, H = 1–5 cm, and ρ = 0.8–1.7 g/cm^3, being its uncertainty below 5%. The efficiency has been checked by the measurement of standards, resulting in a good agreement between experimental and expected activities. The described methodology can be extended to similar situations when samples show geometric and compaction differences.

Keywords: efficiency calibration • environmental radioactivity • gamma spectrometry • geometric dependence of the efficiency • self-attenuation corrections

M. Barrera✉, M. Casas-Ruiz, J. J. Alonso, J. Vidal
Group of Environmental Radioactivity,
Applied Physics Department,
CEIMAR,
University of Cadiz,
Avda. Rep. Saharaui s/n, Puerto Real 11510, Cádiz,
Spain,
Tel.: +34 956 483 419, Fax: +34 956 015 101,
E-mail: manuel.barrera@uca.es

Received: 31 May 2016
Accepted: 7 November 2016

Introduction

The quantitative determination of radionuclides by gamma spectrometry requires the knowledge of the FEPE (full energy peak efficiency, from now in the text just the efficiency). The efficiency depends on the energy, composition, and geometry of sample and detector; their relative position; and the presence of materials between sample and detector (sample container, detector window, dead layer, etc.) [1, 2]. Even though, in most cases, many of these variables are fixed, in practice, it is usual that some of the variables may have a certain degree of variability. It is important to identify at each particular situation the set of variables on which the efficiency is depending and to determine the explicit dependence on these variables, in order to determine the radionuclide activities with the required degree of precision at the specific situation. This precision is in general relatively high when radionuclide activities obtained from gamma spectrometry measurements are used to study environmental processes.

In our case, marine sediments are being measured in order to determine the sedimentation, sediment

transport, and other environmental and geological processes. The number of samples measured in this study is high (namely, hundreds of samples), as they are sediment core sections resulting from many cores being studied (around 25 cores). Sediment samples are measured in cylindrical geometry containers with a constant diameter. However, as it will be described later in detail the studied sediment samples have different masses, so they have different heights. Moreover, samples do not have same compaction, showing a significant variation of densities. Height and density are variables that have a very important effect in the efficiency, and therefore, both variables must be taken into account (besides the energy) in our evaluation of the efficiency. It is very important to indicate that, as it will be shown in the present work, the studied sediment samples do not show significant differences in composition. This fact will allow to calculate and correct the effect produced by the different sample attenuation in terms of the density of the sediment. Otherwise, the effect of composition variability should also be considered in the calibration.

It is necessary then to determine ε as a function of all its variables: the gamma energy E, the sample height H, and its density ρ. The dependence on the energy $\varepsilon(E)$ must be known in order to obtain the activity of radionuclides from its emissions in the whole energetic interval of interest, in our case E = 120–2000 keV. The dependence on the sample height $\varepsilon(H)$ must be determined, as the maximum available quantity of sediment sample has been used in this work to obtain the maximum possible detection of radiation, leading this to a variable sample height, within the interval H = 1–5 cm. Finally, samples do not have the same compaction degree, being their density within the interval ρ = 0.8–1.7 g/cm^3, so the attenuation of the radiation is not expected to be the same for all the samples. This attenuation inside the samples, usually known as self-attenuation, must be studied in order to obtain the dependence on the density $\varepsilon(\rho)$. Therefore, the efficiency calibration in our case consists of the determination of the three variable function $\varepsilon(E,H,\rho)$.

The methodology applied to determine such efficiency calibration is presented in this work, describing in detail the different steps used and the obtained results. First of all, the efficiency $\varepsilon_P(E,H)$ for a sediment P with fixed density will be experimentally determined, as a function of the energy E and sample height H. From this initial calibration, and using the self-attenuation correction depending on the density of the sediment ρ, the efficiency for the whole set of sediment samples $\varepsilon(E,H,\rho)$ will be obtained. Finally, the efficiency is validated by measuring several standard samples containing well-known activities of gamma radionuclides. The results are compared with the ones obtained by the direct calculation of the efficiency (using LabSOCS software). The proposed methodology, based on an empirical basis, provides a lower uncertainty than the calculation methodology, being, therefore, a suitable methodology when the highest precision is required, as it is the case in environmental studies.

Experimental

Sample collection and preparation

Even though the aim of this work is not the description of environmental dispersion of radionuclides in the studied sediments, it is important to explain the methodology used to collect and prepare the samples, in order to count on this information to adequately understand the intention and methodology used to perform the efficiency calibration of the system.

The sediment samples have been extracted from the seabed in different sampling campaigns [3–6] conducted in the area of study, the Bay of Cadiz, located at the Southwestern part of Spain. A relatively high number of stations were studied (25 stations) in order to obtain a precise image of sedimentary process taking place in the area. Cylindrical 1-m long tubes containing the sediment were extracted from the sea bottom by means of a vibrocore system. This allows obtaining the complete column without altering the structure of the sediment. Cores were initially kept at –5°C in laboratory in order to keep undisturbed the interstitial water and the whole structure of the sediment column until the analysis of samples. Later, the sediment columns were sectioned in 2-cm thick slices. Each sample was dried at 70°C during 48 h and then milled and sieved to a grain size finer than 0.5 mm to ensure its homogeneity for the spectrometry measurements.

Sample geometry and density

The measurement of sediment samples has been performed using cylindrical polypropylene containers with inner diameter of 46 mm and thickness of the wall was 0.8 mm. The contained sample height is variable, in the range 10–50 mm, because the sediment quantity contained in the initial core slices is different, depending on the location of the station and the depth of the sedimentary slice, and because most available quantity of sediment has been used for gamma spectrometry measurements, in order to get the maximum possible detection of radiation.

It is very important to control and measure the geometric shape of samples, as the efficiency will strongly depend on such geometry. As the efficiency will be valid for cylindrical geometry, it is necessary, after the sediments are put into the containers, to obtain a top surface of such samples as horizontal as possible. This has been achieved by soft manual rotation of the samples and later by sweeping the sample top face with a straight rule. Once this is done for all the samples, the height H of every sample is measured using a rule graduated in millimetre ($\pm$1 mm).

The parameter H will be used directly as a variable in the calculation of the efficiency. Moreover, H is also used to determine the sample density ρ, which is another variable necessary to determine the efficiency. The sample density has been calculated from its mass m and volume $V = SH$ (S being the sample area), and using $\rho = m/V$. Despite the apparent simplicity of this determination, this method provides

the best possible result in our case, because the density of the sample contained in the final container used to perform the measurement must be known, in order to calculate the self-attenuation corrections because of the compaction degree of samples during the measurement. The obtained density of sediment samples is within the interval 0.8–1.7 g/cm^3.

After the sediments are packed, samples are sealed with paraffin plastic film (Parafilm) and stored for a time period longer than a month, in order to avoid radon ^{222}Rn emanation and to get the equilibrium of the radon (^{222}Rn, $T_{1/2}$ = 3.8 days) with its daughters. The activity of the parent radionuclide ^{226}Ra will be determined by the measurement of the daughters ^{214}Pb and ^{214}Bi, considering the mentioned equilibrium is reached. The measurement of samples has been performed in coaxial position and using the minimum possible distance in relation to the top face of the detector (5 mm), in order to get the maximum possible counting efficiency of the system.

HPGe detector used

Gamma spectrometry measurements have been performed using a coaxial HPGe detector with active volume of 90 cm^3 (50.5 mm in diameter × 46.6 mm in height), relative efficiency of 20%, and resolution of 2 keV at 1332 keV (model: GC2020 CANBERRA). The detector is placed in a cryostat system in order to be cooled at 77 K using liquid nitrogen and is shielded with a 10-cm-thick lead shielding, with internal sheets of Cu and Cd of 1 mm in thickness, to reduce the influence of external background radiation. The detector is sensitive in the 60 keV to 10 MeV energy range. Radionuclides of interest in the posterior measurement of sediment samples (Cs-137, K-40 and U-238, Th-232 series gamma emitters) have emissions in the 120–2000 keV interval, so this will be the energy range of interest to be studied in this work.

Background measurements were performed by measuring an empty container and were carried out periodically (at least once a month) in order to verify the stability of background counting rates. These rates are later subtracted from measurements rates to obtain nuclide activities, being, therefore, very important to check their values keep basically constant inside statistical uncertainties.

The software used to analyse gamma spectra has been varied, depending on the purpose of the measurement. For the measurements of standards that are used to obtain the efficiency calibration, a simple software (Accuspec software) has been used, because we only need to extract the peak areas from these measurements. Later, the analysis of environmental samples spectra is performed using conventional Genie 2000 package software from Canberra.

Experimental determination of the efficiency – previous considerations

The experimental determination of the efficiency is usually performed by the measurement of a standard sample containing different radionuclides with known activities and gamma emissions covering the energy range of interest. Considering the definition of the efficiency ε as the quotient between counted D and emitted N photons

$$\varepsilon = \frac{D}{N} \tag{1}$$

and because the number of photons N emitted during a time t by a radionuclide with activity A for the specific emission with intensity Y is $N = A \cdot Y \cdot t$, the efficiency can be obtained as

$$\varepsilon = \frac{D}{A \cdot Y \cdot t} \tag{2}$$

where the counts D are extracted from the measurement of the standard as the area of the corresponding peak in the spectrum. The efficiency determined by Eq. (2) can only be used for the specific detector used and is only valid for samples with the same geometry, composition, and density than the measured standard, in the energy range considered. The uncertainty associated to the efficiency determined using Eq. (2) comes basically from the counting statistics on D and from the original uncertainty on the activity A. In the case these two sources are small enough then the uncertainty of the intensity Y could also be considered. It is important to reduce the uncertainty of the efficiency determination as much as possible, because this uncertainty is later propagated into the uncertainty of the activity calculated using such efficiency. Uncertainties in this work will be evaluated and expressed at the $k = 1$ ($=1\sigma$) level according to the "Guide to the expression of uncertainty in measurement" – GUM ISO guide [7].

In the specific case of measuring variable size samples by gamma spectrometry, it is necessary to obtain the efficiency of the system as a function of the geometric parameters that define the shape of the sample. In our case, samples have variable height H, so the dependence $\varepsilon(H)$ must be obtained. In order to do so, an experimental method described in detail in next paragraph will be used. The idea used is simple. A standard material will be prepared by spiking a sediment sample with a solution containing a mixture of gamma radionuclides with known activities, emitting a set of gamma energies E_i. Using this material, cylindrical samples of different height H_j will be prepared and measured, in order to obtain the efficiency values $\varepsilon(E_i,H_j)$, at the specific energies E_i and heights H_j. The fit of these values to an adequate function will allow to obtain the efficiency $\varepsilon(E,H)$ valid for the studied range of energy and height.

This method has been used with success by different authors [8, 9]. Bolívar [8] uses it to study soil samples in cylindrical geometry with constant diameter (6.5 cm) and variable height (0–5 cm), in the energy interval of 300–1500 keV, showing that it is possible to express the efficiency as

$$\varepsilon(E,H) = a \cdot E^{-b} \cdot e^{-cH} \tag{3}$$

being a, b, and c are constant parameters obtained from the fitting process and providing the expression a relative uncertainty below 10%. As it will be shown, in our case, the obtained function could be considered an extension of Eq. (3), where b and c are not constant parameters, but functions depending on H, giving our efficiency a relative uncertainty below 5% and being valid in the 100–2000 keV interval.

Efficiency calibration as a function of the energy and sample height $\varepsilon_P(E,H)$

The efficiency for a specific sediment P with density $\rho_P = 1.64$ g/cm^3 has been experimentally determined, as a function of the gamma energy E and the height H of the sample. The sediment was collected during a campaign specifically conducted to obtain superficial (water-sediment interface) sediments, allowing the collection methodology to extract an adequate quantity to be used to general calibration purposes. A standard solution containing a mixture of radionuclides with no coincidence summing effects has been used in order to spike the sediment P. A certain mass of sediment M_P has been spiked with a volume V_S of solution ($M_P = 290.17 \pm 0.01$ g, $V_S = 10 \pm 0.1$ ml) containing the gamma radionuclides. Table 1 shows the radionuclides present in the standard solution, their gamma emissions E_i ($1 \le i \le 6$) and intensities Y_i, and the activities $a_{D,i}$ and $a_{P,i}$, in the solution [Bq/ml] and spiked sediment [Bq/kg], respectively, for the reference date 1 March 2015. The relative uncertainty of the activities in the solution is 3% according to the calibration certificate of the standard.

The homogenization of the solution in the sediment sample P has been achieved by a consecutive application of steps. First, the solution has been mixed in the sample by inserting different layers of sediment and uniformly distributed drops of solution successively, until complete M_P and V_S. Then, the sediment is dried (at 70°C for 48 h). After that, the sediment is transferred to a different container by means of a spoon. During this process, the lumps encountered in the sediment, produced after the drying of the solution, are manually disaggregated with a small rod. Finally, the container is sealed and mechanically agitated.

The correct efficiency calibration requires the correct homogenization of the tracer in the sediment, because a heterogeneous distribution would produce an imprecise efficiency determination, that, therefore, would affect negatively the activity values obtained for all the measured samples using such

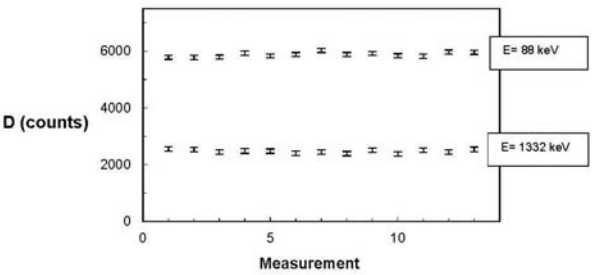

Fig. 1. Counts D for each measurement (for 88 and 1332 keV emissions). The constancy of D shows that the homogenization of the radionuclide solution in the sediment is achieved. The fluctuations of D are only due to the statistical counting.

efficiency. Considering the crucial importance of this issue, the homogenization has been verified by measuring the prepared standard for several times and shaking the standard in a strongly way during 10 min before performing each measurement. The standard was measured a total of 13 times, being 2 h the acquisition time, in order to reduce the counting statistical uncertainty below 1% for all the gamma emissions. Figure 1 represents the counts D of the minimum and maximum gamma emissions energies of the standard, 88 and 1332 keV, respectively, for all the measurements, showing the constancy of counts D for both emissions.

If the homogenization is actually reached, it is expected that the only source of fluctuations of D displayed in Fig. 1 is the counting statistics. It has been determined the statistical standard deviation s of counts D for each energy, being $s(88\text{ keV}) = 60 \pm 12$ and $s(1332\text{ keV}) = 78 \pm 16$, and also the statistical counting uncertainty of single measurements (represented by the error bars), being $\sigma(88\text{ keV}) = 71.4 \pm 0.5$ and $\sigma(1332\text{ keV}) = 77.8 \pm 0.5$. The total agreement of the standard deviation and the counting uncertainty (for every emissions, not only for these two) show clearly that it has been achieved the homogenization of the spiked radionuclides in the sediment. A heterogeneous distribution would produce a deviation $s > \sigma$, especially for the 88-keV emission, because as the sample attenuation is higher at low energy, the counting D is, therefore, expected to be much more sensitive to any possible heterogeneity for this lower energy.

Once homogenization has been achieved, five samples P_j, $1 \le j \le 5$, with heights H_j, where $j = 1$, 2, 3, 4, 5 cm, have been prepared using the same standard plastic container (diameter 4.60 ± 0.01 cm) used for the measurement of the generic sediment samples. The measurement of standards P_j has been

Table 1. Gamma energy, intensity, half-life, and activities (in original solution and spiked sediment P at the reference date 1 March 2015) of radionuclides used to determine the efficiency for sample P. Relative uncertainty of activity is 3%

Radionuclide	$T_{1/2}$ [days]	E [keV]	Y [%]	a_D [Bq/ml]	a_P [Bq/kg]
^{109}Cd	462.3	88	3.6	100.9	3480
^{57}Co	271.8	122	85.5	4.8	164.8
^{57}Co	271.8	136	10.7	4.8	164.8
^{137}Cs	1095.0	662	85.2	15.0	517.8
^{60}Co	1923.9	1173	99.9	22.9	789.4
^{60}Co	1923.9	1332	99.9	22.9	789.4

performed using different counting times t_j, being longer for smaller samples (48 h for P_5, 7 days for P_1) in order to reduce statistical uncertainty of every peak area below 1% (except for the energy E_3 = 136 keV, being 5% the uncertainty for this area, because of the low available activity of radionuclide ^{57}Co and also to the low intensity of this gamma emission).

The counts D_{ij} for the emission E_i of the measured standard P_j (having height H_j and mass m_j) are

$$D_{ij} = \varepsilon_{ij} \cdot a_{Pi} \cdot m_j \cdot Y_i \cdot t_j \tag{4}$$

where ε_{ij} is the efficiency for the energy E_i and sample height H_j. Therefore,

$$\varepsilon_{ij} = \frac{D_{ij}}{a_{Pi} \cdot m_j \cdot Y_i \cdot t_j} \tag{5}$$

This expression allows determining the efficiency values ε_{ij}, using the measured peak areas D_{ij} (energy E_i of sample measurement with height H_j) and the rest of known parameters. Even though it is possible to perform these calculations in a more automated way using specific software packages (e.g., Genie 2000), the manual determination presented has been used, extracting individual peak areas from each spectrum and applying the previous expression. This methodology allows a much more direct control of different variables that are used to calculate the efficiency, which is not generally possible when such specific programs are used.

Table 2 shows the obtained values ε_{ij}^{exp} [%] = $100\varepsilon_{ij}^{exp}$, where exp denotes that they have been experimentally determined. The relative uncertainty of the efficiency comes basically from the original uncertainty of the activity nuclides (3%) and also from the spiking (1%) and counting statistics (<1%), being this uncertainty of the efficiency 3.5%, except for the energy E_3 = 136 keV, being in this case 6%, because of the previously mentioned reasons for this particular emission.

The values shown in Table 2 can be used directly as the efficiency values for a P type sediment (ρ_P = 1.64 g/cm^3), for every one of the particular energies and heights specified by rows and columns. However, the gamma energies that will be measured later in sediment samples do not coincide in general with the energy values E_i of the used standard and the height of these samples neither will have in general a value $H_j = j$ cm. Therefore, it is necessary to determine from these experimental values ε_{ij}^{exp} a fitting function $\varepsilon_P(E,H)$ that could be used in a whole range of energy E and height H.

Figure 2 represents $\ln(\varepsilon^{exp})$ in function of $\ln(E)$, considering E in kiloelectronvolts. For every height,

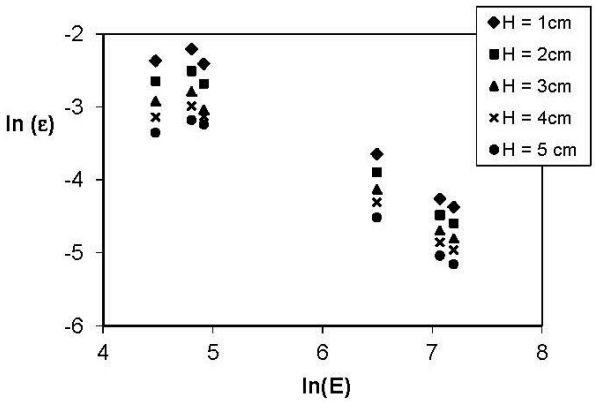

Fig. 2. Experimental values of $\ln(\varepsilon)$ vs. $\ln(E)$, for each sample height H. The $\ln(\varepsilon)$–$\ln(E)$ relationship is linear for energies higher than E = 122 keV ($\ln(E)$ = 4.8).

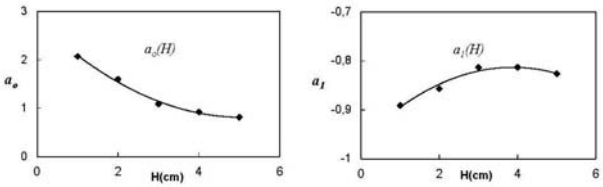

Fig. 3. Parameters a_0 and a_1 vs. the height H. Continuous lines represents the fitting functions.

the characteristic linear relationship between $\ln(\varepsilon)$ and $\ln(E)$ can be observed, existing a deviation from this linearity at the lower energy (E_1 = 88.03 keV), as it is usual for germanium detectors. Therefore, a linear expression is proposed for every height H_j

$$\ln(\varepsilon_j) = a_{0j} + a_{1j} \ln(E) \tag{6}$$

valid for $E \geq E_2$ = 122 keV. Coefficients a_{0j} and a_{1j} have been obtained from the least squares fit and are shown in Table 3, together with the correlation and χ^2 values.

Figure 3 represents the coefficients a_0 and a_1 in a function of the height H, exhibiting an approximately linear dependence in both cases, with a small curvature for higher H. Therefore, a 2° order polynomial for each one of these coefficients has been proposed

$$\begin{aligned} a_0(H) &= m_0 + m_1 \cdot H + m_2 \cdot H^2 \\ a_1(H) &= n_0 + n_1 \cdot H + n_2 \cdot H^2 \end{aligned} \tag{7}$$

Parameters m_k and n_k, $0 \leq k \leq 2$, obtained from the least squares fits are shown in Table 4 (valid for H [cm]) together with the correlation coefficients. Obtained fitting functions $a_0(H)$ and $a_1(H)$ are represented in Fig. 3.

Table 2. Experimental values of the efficiency ε_P [%] for each sample height and gamma energy

E [keV]	H_1 = 1 cm	H_2 = 2 cm	H_3 = 3 cm	H_4 = 4 cm	H_5 = 5 cm
88	9.40	7.09	5.39	4.35	3.51
122	11.04	8.15	6.18	5.05	4.18
136	9.01	6.86	4.80	4.38	3.92
662	2.62	2.03	1.62	1.35	1.09
1173	1.41	1.13	0.92	0.78	0.65
1332	1.27	1.01	0.82	0.70	0.58

Table 3. Values of fit parameters a_0 and a_1, correlation coefficient r, and χ^2 for each sample of height H_j

	H_1 = 1 cm	H_1 = 2 cm	H_1 = 3 cm	H_1 = 4 cm	H_1 = 5 cm
a_0	2.07	1.59	1.08	0.91	0.81
a_1	–0.89	–0.86	–0.81	–0.81	–0.83
r	0.999	0.999	0.998	0.999	0.999
χ^2	0.74	0.60	1.17	0.41	0.58

Table 4. Values of fit parameters m_k and n_k, $0 \le k \le 2$, (H [cm]) and correlation coefficient

a_0 :	$m_0 = 2.775$	$m_1 = -0.7586$	$m_2 = 0.07315$	$r(a_0) = 0.995$
a_1 :	$n_0 = -0.9603$	$n_1 = 0.07488$	$n_2 = -0.00959$	$r(a_1) = 0.999$

Table 5. Deviation δ [%], between theoretical and experimental values of ε_P [%]. Lower row shows the deviation for the specific calibration at 662 keV

E [keV]	H_1 = 1 cm	H_2 = 2 cm	H_3 = 3 cm	H_4 = 4 cm	H_5 = 5 cm
122	–0.78	–2.14	–0.81	–1.51	1.85
136	4.51	4.13	4.82	3.51	–1.10
662	–5.84	–6.60	–2.57	–6.17	–2.91
1173	2.24	3.31	3.72	0.60	1.32
1332	1.90	3.52	4.49	1.29	2.27
662	–1.20	1.30	1.30	–2.30	0.80

Table 6. Fit parameters and correlation coefficient for the efficiency function at the specific energy 662 keV

$c_0 = 3.22 \times 10^{-2}$	$c_1 = -6.83 \times 10^{-3}$	$c_2 = 5.20 \times 10^{-4}$	$r = 0.999$

Combining fit expressions (6) and (7), we obtain

$$\varepsilon_P^*(E,H) = e^{a_0(H)} \cdot E^{a_1(H)} \tag{8}$$

This function provides the efficiency as a function of the gamma energy E and the height H of the samples, being valid in the range $122 \le E$ [keV], ≤ 1332, $1 \le H$ [cm], ≤ 5, and for P type sediments, that is, for samples with density of $\rho_P = 1.64$ g/cm^3, or similar. Moreover, the strong linear relationship between $\ln(\varepsilon)$ and $\ln(E)$, displayed in Fig. 2, will allow to use the expression at energies higher than 1332 keV, as it will be shown later when the efficiency is checked.

In order to estimate the accuracy of expression (8), the deviation $\delta(\varepsilon_P^*)_{ij}$ between experimental ε_{ij}^{exp} and theoretical values provided by $\varepsilon_P^*(E,H)$ has been determined, being $\delta(\varepsilon_P^*)_{ij}$ defined as

$$\delta(\varepsilon_P^*)_{ij} = \frac{\varepsilon_P^*(E_i,H_j) - \varepsilon_{ij}^{exp}}{\varepsilon_{ij}^{exp}} \tag{9}$$

Deviations $\delta(\varepsilon_P^*)_{ij}$ are shown in Table 5, being the higher values for E_3 = 136 keV (^{57}Co) and for E_4 = 662 keV (^{137}Cs). If this last emission is not considered for now, it can be concluded that $\delta(\varepsilon_P^*)_{ij} \le 5\%$.

As ^{137}Cs is one of the radionuclides that will be later determined in sediments, it is interesting to perform a specific calibration for the energy E_3 = 662 keV that will obviously depend only on the sample height and that will be denoted by $\varepsilon_p^{Cs}(H)$. Figure 4 represents experimental efficiency for 662 keV, as a function of the sample height H, being the relationship approximately linear, but having some degree of curvature. Therefore, it is proposed for $\varepsilon_p^{Cs}(H)$ a 2° order polynomial in H

$$\varepsilon_P^{Cs}(H) = c_0 + c_1 \cdot H + c_2 \cdot H^2 \tag{10}$$

Table 6 shows the coefficients c_k, $0 \le k \le 2$, determined by the least squares fit, together with the achieved correlation. Deviation between experimental and theoretical values provided by $\varepsilon_p^{Cs}(H)$, shown in Table 5, are significantly smaller than the obtained using $\varepsilon_p(E,H)$, justifying, therefore, the specific calibration performed for the energy 662 keV.

Finally, the efficiency calibration for a sediment sample P (ρ_P = 1.64 g/cm^3) is the function $\varepsilon_P(E,H)$ defined as

$$\varepsilon_P(E,H) = \left\{ \begin{array}{l} \varepsilon_P^*(E,H) \\ 122 \le E\,[\mathrm{keV}] \le 1332, \\ E \ne 662\,\mathrm{keV} \\ \varepsilon_P^{Cs}(H) \\ E = 662\,\mathrm{keV} \end{array} \right\} 1 \le H\,[\mathrm{cm}] \le 5 \tag{11}$$

being its relative uncertainty below 5%.

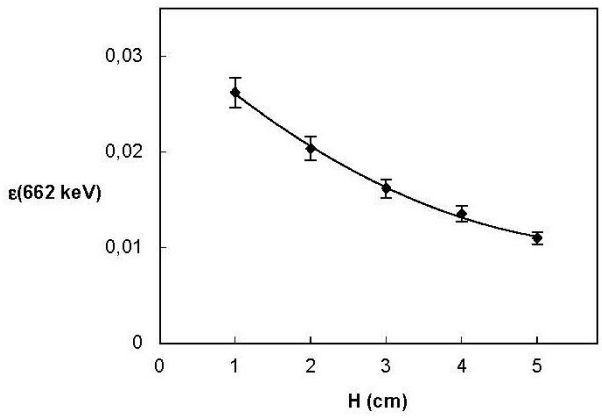

Fig. 4. Efficiency at the specific energy of 662 keV vs. the height H. Continuous line represents the fitting function.

Mass attenuation coefficient of sediment samples

In order to calculate the self-attenuation corrections of the previously determined efficiency, required because of the different degree of compaction of samples in relation to the standard, it is necessary first of all to determine the attenuation of the whole set of sediment samples. The study of the attenuation of gamma radiation in materials is performed using the 'linear attenuation coefficient' μ, defined for homogeneous materials as the probability of interaction per unit of length. The intensity of a photon beam I_o crossing a material with thickness x is reduced to the value $I = I_o\varepsilon^{-\mu x}$, from where the quotient of intensities is derived, defined as the transmission T that represents the ratio of photons that do not interact in the material

$$T = \frac{I}{I_o} = e^{-\mu x} \tag{12}$$

The linear attenuation coefficient μ depends on the composition of the material and on its density ρ, besides the energy of the radiation. In order to remove the dependence on the density, the 'mass attenuation coefficient' defined as $\mu_{mas} = \mu/\rho$ is introduced. It can be shown that μ_{mas} actually depends on the elemental composition of the material but not on its density. If the elemental composition of the material is known, it is possible to calculate μ_{mas} by summing the contribution of every atomic species, and taking into account that the coefficient is tabulated for the different atomic species [10].

When the composition of a sample is unknown, it is possible to determine the attenuation experimentally by measuring the transmission of photons T emitted from a point-like source and using expression (12). In order to do this, it is important to place the source at a distance away enough from the sample and detector, so that the hypothesis of normal incidence of radiation is fulfilled, and therefore, the path x of photons across the sample can be considered as the sample height H. Moreover, moving away the source from the detector, coincidence summing effects can be avoided in case a multienergetic gamma emitter is used as the source. The transmission method allows to determine $\mu(E_k)$ and $\mu_{mas}(E_k) = \mu(E_k)/\rho$, for every energy E_k emitted by the source so that, if it is necessary to know the attenuation for a complete energy interval, these values can be fitted to an appropriate function $\mu(E)$ or $\mu_{mas}(E)$, respectively.

Using this methodology, the mass attenuation coefficient μ_{mas} of the sediment samples has been determined. In order to do so, the transmission T of photons has been measured for a total of six sediment samples with densities within the interval 0.8–1.7 g/cm^3, that is, covering the density interval of the whole set of samples studied. Measurements were performed using a point-like source containing ^{152}Eu, placed at 25 cm from the detector, in order to avoid coincidence summing effects and also to produce the photon incidence on the sample and detector as normal as possible, as previously described. In order to reduce statistical uncertainty for the measurement of photon intensities I, I_o below 1%, counting time has been set to 24 h.

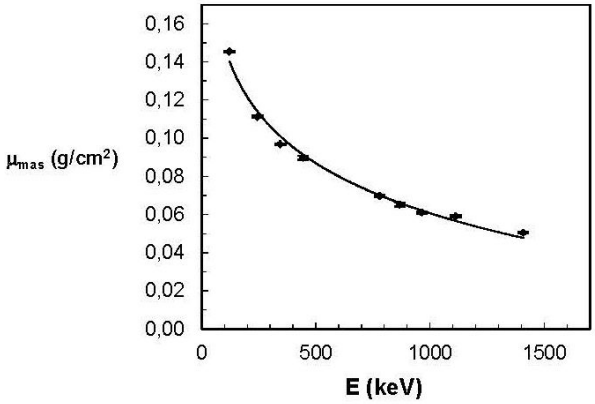

Fig. 5. Mass attenuation coefficient for sediment samples vs. energy. The represented size of the experimental point includes the values of the attenuation for the different measured samples, showing that a common mass attenuation coefficient exists for the set of sediment samples.

Figure 5 shows the mass attenuation coefficient μ_{mas} as a function of the gamma energy E, obtained for the six measured samples. The uncertainty of μ_{mas} has been determined using the standard propagation rules [7], considering the uncertainty of each variable used to calculate the attenuation, that is, the counting statistics of I and I_o, and the uncertainty in the determination of sample height H and density ρ. The obtained relative uncertainty for μ_{mas} is below 5%. For each gamma energy, the small variations of μ_{mas} for the set of different densities do not show any relationship with the density, being, moreover, these variations inside the uncertainty interval, showing then that the value of μ_{mas} do not depend on the sample density, as it is in fact displayed by Fig. 5.

Therefore, there is a common mass attenuation coefficient associated to the whole set of sediment samples studied, what is probably because of the fact that the samples belong to the same geographical area and, therefore, have very similar composition, with minor variations, producing then this homogeneity in composition the same attenuation. Table 7 shows the average values of μ_{mas} for each measured energy. There is a strong linear correlation (r = 0.997) between μ_{mas} and $\ln(E)$, so that the values can be fitted through the expression

$$\mu_{mas}(E) = q_1 + q_2 \ln(E) \tag{13}$$

Table 7. Mass attenuation coefficient of sediment samples determined by the measurement of photon transmission using a point-like source of ^{152}Eu

E [keV]	μ_{mas} [cm^2/g]
122	0.145 ± 0.004
245	0.111 ± 0.003
344	0.096 ± 0.002
444	0.089 ± 0.004
779	0.069 ± 0.003
867	0.065 ± 0.005
964	0.061 ± 0.002
1112	0.059 ± 0.002
1408	0.050 ± 0.002

where $q_1 = 3.24 \times 10^{-1}$ and $q_2 = -3.81 \times 10^{-2}$ (for E [keV] and μ_{mas} [cm^2/g]). The shape of the fitting function is represented as the continuous line in Fig. 5.

As the sediment samples studied have densities within the interval 0.8–1.7 g/cm^3, the linear attenuation μ is, therefore, higher for the most dense samples. For every sample M having a density ρ_M, the linear attenuation is then

$$\mu_M(E) = \rho_M \cdot \mu_{mas}(E) \quad (14)$$

It must be indicated that the existence of a common value of μ_{mas} for a set of samples extracted from a determined environment is not always fulfilled. In particular, this common coefficient does not exist when samples show very different compositions or when there are high variations in the granulometry among the samples [11].

Self-attenuation corrections

Definition of the self-attenuation correction factor

The study of the efficiency dependence on its variables can be performed in a direct experimental way when the number of such variables is not high, as $\varepsilon_P(E,H)$ has been obtained. However, when the number of variables is high, in practice bigger than 2, it is very difficult to obtain the efficiency in a strictly experimental way, because of the multiplicity of possibilities and the complexity related to reproduce such situations in a laboratory.

In that case, the determination can be performed with an initial experimental stage, measuring standard samples, and the subsequent application of theoretical factors that correct for the variation of the efficiency produced by the additional variables. This empirical-theoretical methodology allows extending the validity of the efficiency toward a bigger applicability range, achieving, therefore, a compromise solution between the precision of the experimental determination and the scope reached by the theoretical methods.

In particular, the use of the efficiency for samples with different density or composition can be performed by the determination of the self-attenuation correction factor, defined as follows. Let suppose two samples M and P having a different attenuation (because of different composition and/or density) but having the same geometry and being measured at the same relative position to the same detector. The efficiencies ε_M and ε_P associated to M and P, respectively, are not equal in general, because of the different attenuation of radiation inside the samples. The objective of the self-attenuation correction is the determination of the unknown efficiency ε_M associated to the generic attenuation sample M, starting from the known efficiency ε_P. In order to do so, the self-attenuation correction factor of the sample M in relation to the sample P is introduced as

$$F_{MP} = \frac{\varepsilon_M}{\varepsilon_P} \quad (15)$$

The determination of F_{MP} is somehow equivalent to the determination of the efficiency, being performed in practice by proposing a simplified model for the efficiency. The precision of the factor is conditioned to the ability of the model to reproduce the variability of the efficiency, more than to the precision in the estimation of the efficiency itself, as the deviation between the real and theoretical values will tend to cancel in the quotient (15). Taking into account the definition of efficiency $\varepsilon = D/N$, expression (15) is equivalent to

$$F_{MP} = \frac{D_M}{D_P} \quad (16)$$

That is, the self-attenuation correction can be understood as the fraction of photons detected for sample M with respect to P, supposing the activity of both samples is the same and, therefore, are emitting the same number of photons N.

Moreover, the self-attenuation correction of samples M and P with respect to a hypothetical nonattenuating sample O can be defined as $F_{MO} = \varepsilon_M/\varepsilon_O$, $F_{PO} = \varepsilon_P/\varepsilon_O$. This allows writing F_{MP} as a quotient of these self-attenuation factors with respect to a nonattenuating sample

$$F_{MP} = \frac{F_{MO}}{F_{PO}} \quad (17)$$

Expressions (15)–(17) are equivalent and useful when the calculation of self-attenuation correction must be performed. Once F_{MP} has been calculated and the standard P efficiency ε_P has been measured, the efficiency ε_M can be determined as

$$\varepsilon_M = F_{MP} \cdot \varepsilon_P \quad (18)$$

If corrections are not applied, the direct use of the efficiency ε_P introduces a systematic error in the efficiency, being, therefore, in such case this error propagated into the activity of samples. Anyway, the correction only makes sense when it produces a significant modification of the efficiency ε_P, of similar or higher value than its relative uncertainty, that is, we can prescind from F_{MP} when there is a reduced variability of ε_M with respect to ε_P.

Cutshall correction

Among the different approximations that have been developed to estimate the self-attenuation correction, the expression introduced by [12] is the most used because of its simplicity and acceptable degree of precision. This factor can be used for cylindrical samples coaxially centred with the detector, being a valid approximation when the sample height is not large compared to the dimensions of the detector, as it is our case. If sample dimensions are too large, the Cutshall correction could lead to imprecise results, being necessary in such cases to use other more sophisticated and precise correction factors [13, 14].

The Cutshall self-attenuation factor F_{MO} for a sample M with respect to a nonattenuating sample O is

(19) $$F_{MO} = \frac{1 - e^{-\mu_M \cdot H}}{\mu_M \cdot H}$$

where μ_M is the linear attenuation coefficient at the considered gamma energy and H is the height of the sample. As M is a generic sample, the previous expression is valid for sample P (writing P instead of M), so using Eq. (17), the Cutshall self-attenuation correction factor F_{MP} of sample M with respect to sample P is obtained

(20) $$F_{MP} = \frac{\dfrac{1 - e^{-\mu_M \cdot H}}{\mu_M \cdot H}}{\dfrac{1 - e^{-\mu_P \cdot H}}{\mu_P \cdot H}} = \frac{\mu_P}{\mu_M} \cdot \frac{1 - e^{-\mu_M \cdot H}}{1 - e^{-\mu_P \cdot H}}$$

In order to calculate F_{MP}, it is necessary to know the attenuation coefficient μ of samples M and P, what can be determined by measuring the transmission T, as it has been described and performed for the sediment samples.

Correction factor of the studied sediment samples

In order to obtain the efficiency ε_M valid for a generic sediment sample M starting from the experimentally determined efficiency ε_P of the standard P, with density $\rho_P = 1.64$ g/cm^3, self-attenuation correction factor (20) has been used. Considering that the linear attenuation coefficient μ of samples M and P can be expressed in terms of a common mass attenuation coefficient $\mu_{mas}(E)$, expression (14), the correction factor turns to

(21) $$F_{MP}(E,H,\rho_M) = \frac{\rho_P}{\rho_M} \cdot \frac{1 - e^{-H\rho_M \cdot \mu_{mas}(E)}}{1 - e^{-H\rho_P \cdot \mu_{mas}(E)}}$$

where $\rho_P = 1.64$ g/cm^3 and $\mu_{mas}(E)$ has been previously determined and is given by Eq. (13). The correction, therefore, depends explicitly on three variables: gamma energy E, sample height H, and sample density ρ_M. In order to study the magnitude of F_{MP} and the way it depends on its variables, F_{MP} (Fig. 6) in function of every one of its variables has been represented, keeping the value of the two other variables constant. The constant values selected have been $E_o = 122$ keV, $H_o = 5$ cm, and $\rho_{Mo} = 0.8$ g/cm^3, corresponding to the minimum E, maximum H, and minimum ρ_M values were reached by the efficiency variables, respectively. These values produce the highest corrections, because the values $E_o = 122$ keV and $H_o = 5$ cm lead to the higher possible attenuation, and $\rho_{Mo} = 0.8$ g/cm^3 provides the higher density difference with respect to the standard P.

Figure 6 shows that the value of the correction factor is above the unit, what is due to the fact that generic samples M have a lower density than the standard P, being, therefore, the counting and associated efficiencies higher for M than those for the standard P. The decreasing shape of $F_{MP}(E,H_o,\rho_o)$ is due to the decreasing effect of attenuation as the energy E increases. The correction is above 5% in the whole energetic range, exceeding 15% for $E < 700$ keV. The increasing shape of $F_{MP}(E_o,H,\rho_o)$

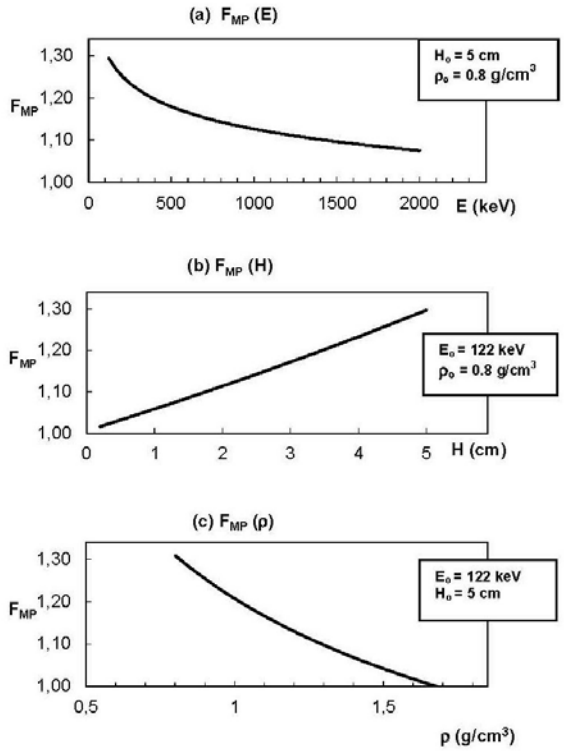

Fig. 6. Self-attenuation correction factor of sediment samples vs. each variable. (a) Dependence on E. (b) Dependence on H. (c) Dependence on ρ.

is due to the increasing effect of the attenuation as the sample is thicker, being the correction above 5% for $H > 1$ cm and exceeding 15% for $H > 3$ cm. With regard to the dependence on the density, $F_{MP}(E_o,H_o,\rho)$ is decreasing, tending to 1 as the density of the sample approaches the density of the standard, $\rho_P = 1.64$ g/cm^3, showing that correction effect disappears as the sample density tends to standard density, because in that case samples M and P have the same degree of attenuation. The correction is above 5% for $\rho_M < 1.4$ g/cm^3, exceeding 15% for $\rho_M < 1.1$ g/cm^3.

As it has been shown, self-attenuation effect is important when compared to the relative uncertainty of the efficiency, estimated as 5%, because the correction values are in the interval 15–30% for a wide part of its applicability range. If corrections were not performed, a very significant systematic error would be introduced in the efficiency calibration, affecting negatively the quality of the activity determinations. Therefore, self-attenuation corrections are necessary in order to not add such an extra source of error and to keep uncertainty as low as possible, 5%.

Sample-detector system efficiency $\varepsilon_M(E,H,\rho_M)$

The searched efficiency of the sample-detector system for a generic sediment sample with density ρ_M and height H at the gamma energy E is

(22) $$\varepsilon_M(E,H,\rho_M) = F_{MP}(E,H,\rho_M) \cdot \varepsilon_P(E,H)$$

where $\varepsilon_P(E,H)$ is given by expression (11) and $F_{MP}(E,H,\rho_M)$ is the self-attenuation correction factor (21). This efficiency function is valid in the range

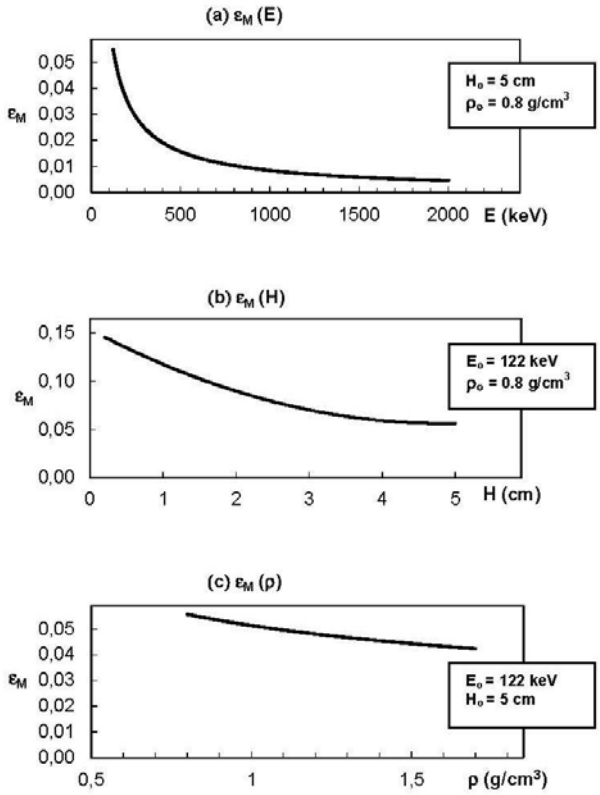

Fig. 7. Sample-detector system efficiency vs. each variable. (a) Dependence on E. (b) Dependence on H. (c) Dependence on ρ.

E = 120–2000 keV, H = 0–5 cm, ρ_M = 0.8–1.7 g/cm^3, in which the measured gamma emissions as well as the studied samples are contained. Relative uncertainty associated to the efficiency is 5%, coming basically from the original uncertainty on ε_P. This uncertainty value will be used later, together with the counting statistics, to determine the final uncertainty on the activity of the measured sediment samples.

Figure 7 represents ε_M in function of each one of its variables, keeping constant the value of the two other variables, as it was performed with F_{MP}. The figure shows the strong dependence of ε_M on the energy, being the variation undergone by the ε_M values between the limits of the energetic interval of one order of magnitude. The dependence of ε_M on the sample height is also very important, producing H a variation that reduces ε_M to a third part of its initial value in the interval H = 0–5 cm. Finally, the dependence of ε_M on the density produces a relative variation of 30%, because of the mentioned effect of the self-attenuation. The significant variation of the efficiency with respect to the studied variables justifies, therefore, the need to perform the calibration in function of these variables.

Validation of the efficiency

In order to validate the efficiency calibration, the measurement of standard samples containing known activities of gamma radionuclides has been performed. These known activity values agree, inside the experimental uncertainties, with the activity obtained from the measurement of samples and using the studied efficiency, showing, therefore, the validity of the efficiency.

Five different standard samples have been considered. First of all, a soil sample supplied by the IAEA (reference material IAEA-SOIL6) containing certified activity values of ^{226}Ra and ^{137}Cs radionuclides has been measured. From this material, a 5-cm height sample has been prepared, being its density 0.98 g/cm^3. In order to ensure secular equilibrium between ^{226}Ra and its daughters, sample measurement was performed one month after its preparation. Counting time was set as 48 h, to reduce statistical uncertainty below 5%. ^{226}Ra determination was performed by measuring the 352 keV and 35% intensity emission (from ^{214}Pb), being necessary to subtract the area corresponding to the environmental background. ^{137}Cs was determined by measuring its 662 keV (85% intensity emission).

According to the sample certificate, the activity values are $a(^{226}\text{Ra})$ = 79 ± 4 and $a(^{137}\text{Cs})$ = 36.5 ± 1.3 Bq/kg. The performed measurement provides a result $a(^{226}\text{Ra})$ = 75 ± 6 and $a(^{137}\text{Cs})$ = 34 ± 3 Bq/kg. A good agreement, inside experimental uncertainties, is, therefore, found between measured and expected activities.

Second, standard samples have been prepared using high-purity compounds such as KCl and $K_2Cr_2O_7$, containing, therefore, the radionuclide ^{40}K. Considering the isotopic fraction (0.01167 ± 0.00004)% and the half-life ($T_{1/2}$ = (1.29 ± 0.02) × 10^9 years) of radionuclide ^{40}K, it can be deduced that the activity a of a generic compound containing potassium is

$$a = 1.21 \cdot 10^6 \frac{q}{M} \text{ [Bq/kg]} \qquad (23)$$

where q is the number of potassium atoms per molecule and M is the molecular weight [u.a.m.]. Such expression provides the activity values of the compounds used, being a(KCl) = (1.66 ± 0.02) × 10^4 and $a(K_2Cr_2O_7)$ = (8.23 ± 0.13) × 10^3 Bq/kg.

Using these compounds, samples with different height have been prepared and measured. The de-

Table 8. Experimental and expected values of radionuclide ^{40}K activity in potassium compounds measured using variable height samples

H [cm]	a(KCl) [Bq/kg] × 10^4	$a(K_2Cr_2O_7)$ [Bq/kg] × 10^3
1	1.65 ± 0.09	8.31 ± 0.70
2	1.57 ± 0.10	8.03 ± 0.90
3	1.61 ± 0.09	8.22 ± 0.60
4	1.65 ± 0.10	8.15 ± 0.55
Expected activity	1.66 ± 0.02	8.23 ± 0.13

termination of ^{40}K has been performed by measuring its 1460 keV gamma emission (intensity 10.7%), subtracting the background area contribution. Acquisition times have been selected between 3 and 24 h, depending on the sample mass, in order to reduce the counting uncertainty below 1% in all cases. The activity values obtained from each measured sample, shown in Table 8, agree with the theoretical activity values calculated for these compounds, within the experimental uncertainties.

It is important to indicate that the attenuation of the standard samples measured to check the efficiency validity is different from the attenuation of the sediment samples, because the composition of such materials is different. In order to calculate the adequate self-attenuation correction of the efficiency, F_{MP}, it has been necessary to determine the attenuation coefficient $\mu_{mas}(E)$ for such materials used to check the efficiency. The methodology used has been exactly the same as in the case of sediments, that is, the measurement of photon transmission using a point-like source of ^{152}Eu has been performed and then the values have been fitted to a function similar to Eq. (13) (but having another fit coefficients, depending on the material composition) to obtain $\mu_{mas}(E)$. The differences found between the values of the attenuation coefficient of the materials used and the corresponding to sediment samples is significant, especially for low energies (around 100%), justifying, therefore, the separated determination of this attenuation. Once the linear attenuation $\mu_M(E)$ of these materials has been determined, $\mu_M(E) = \rho_M \cdot \mu_{mas}(E)$, it is inserted in expression (20), in order to calculate the self-attenuation correction factor F_{MP} for these specific materials. This factor is used to determine the correct efficiency, $\varepsilon_M = F_{MP} \cdot \varepsilon_P$, finally used to obtain the experimental activity from the measurements of these materials.

Finally, two certified reference materials (CRMs) supplied by the IAEA were used to check the proposed calibration: IAEA-385 (sea sediment) and IAEA-444 (soil sample). Details on matrix, preparation, and nuclide activities of these materials are described in [15] (IAEA-385) and [16] (IAEA-444). Two cylindrical samples with heights H = 1 cm and H = 5 cm were prepared and measured using each one of these materials. Measured radionuclides were ^{226}Ra (^{214}Pb), ^{137}Cs, ^{60}Co, and ^{40}K. Counting time was set to 24 h, in order to reduce statistical uncertainty below 5%. Table 9 shows the certified activity values, sorted by nuclide energy, and the activity values obtained using the proposed calibration, together with the deviation [%], between these certified and obtained values. Deviations are below 10% in all cases, improving for H = 5 cm in relation to H = 1 cm, what could probably be due to the higher counting for H = 5 cm samples and the subsequent lower counting uncertainty for all nuclide lines.

In order to compare these results with an alternative calibration methodology, efficiency calculations for these two CRMs were performed using LabSOCS software [17]. To perform these calculations, the mass attenuation coefficients for CRMs were measured (as previously described in this work) and

Table 9. Certified activities for CRMs IAEA-385 and IAEA-444, and experimental values obtained for different size of samples using the proposed calibration and the efficiency calculated using LabSOCS software. Deviations [%] between experimental and certified values are shown to compare both calibrations

Radionuclid	CRM	E [keV]	H = 1 cm						H = 5 cm			
			Certified	Proposed calibration		LabSOCS calibration			Proposed calibration		LabSOCS calibration	
			a [Bq/kg]	a [Bq/kg]	Dev. [%]	a [Bq/kg]	Dev. [%]		a [Bq/kg]	Dev. [%]	a [Bq/kg]	Dev. [%]
^{226}Ra	IAEA-385	352	21.9(0.6)	24.0	**9.5**	17.3	21		23.7	**8.2**	17.7	19
^{137}Cs	IAEA-385	662	33.0(0.6)	30.3	**8.2**	38.0	15		30.6	**7.3**	38.9	18
^{137}Cs	IAEA-444	662	68.5(1.4)	62.7	**8.5**	58.2	15		63.4	**7.4**	58.9	14
^{60}Co	IAEA-444	1173	82.6(2.0)	88.9	**7.6**	69.4	16		87.9	**6.4**	70.2	15
^{40}K	IAEA-385	1461	607.0(6.0)	556.0	**8.4**	728.4	20		563.3	**7.2**	710.2	17

introduced in the software, besides the geometry, shape, dimensions, and general parameters for sample and detector configuration. Table 9 shows the activity values obtained using this calculated efficiency and also the deviations [%] with respect to the certified values. These deviations are higher than those obtained using the proposed calibration, being, in general, bigger approximately by a factor 2 than the deviations obtained via the proposed calibration. The proposed calibration, based on an experimental determination, therefore, improves noticeably the results obtained by LabSOCS calculations.

This validation confirms that the proposed calibration methodology provides a precise efficiency that is required to determine the activity of radionuclides with an uncertainty as low as possible, in order to use such nuclide activities to perform precise environmental studies. Moreover, the agreement found between experimental and expected activities for radionuclide ^{40}K shows that it is possible to extend the applicability of the calibration to energies values higher than the maximum energy of the originally used standard (1332 keV), because of the strong linear relationship existing between $\ln(\varepsilon)$ and $\ln(E)$, displayed in Fig. 2.

Conclusions

A methodology that allows to determine the FEPE $\varepsilon(E,H,\rho)$ for gamma spectrometry measurements with HPGe detector in cylindrical geometry has been developed and applied, being valid when this efficiency depends on the energy of the radiation E, the height of the sample H, and also its density ρ. The method consists of an initial experimental calibration as a function of E and H, using a standard spiked sediment P of fixed density ρ_P, and the application of a self-attenuation factor, depending on the density of the sample ρ, in order to correct for the different attenuation of the generic sample in relation to the measured standard. The efficiency can be used for the measurements of sediments in the whole range of interest studied, E = 120–2000 keV, H = 1–5 cm, ρ = 0.8–1.7 g/cm^3, being its relative uncertainty below 5%.

Even though this calibration has been performed for a particular detector and a specific set of samples, the described methodology could be extended and applied to similar situations, that is, when samples to be measured have geometric differences and also show a different degree of compaction, having a similar composition. From the experimental point of view, besides the preparation and measurement of the standard, in order to be apply the method, the attenuation of samples must be determined by the measurement of photon transmission through material being studied. The attenuation is used to calculate the self-attenuation correction and is also needed to show that a common mass attenuation coefficient exists for the set of samples studied. It is also advisable to check the obtained efficiency by the measurement of different standards with variable geometry and densities covering the studied range. In our case, a good agreement between experimental and expected activities is found when different standards are measured, including CRMs. The results obtained using the proposed calibration are more precise than the ones obtained by using LabSOCS calibration software, showing that specific experimental calibration is still necessary when the lowest uncertainties in measurements are required.

The demonstration of the significant variation of the self-attenuation correction and the efficiency as a function of its variables has also been included as a fundamental part of the method. The study of this variation should be performed in every particular situation, in order to justify the need to calibrate as a function of the considered variables. When the variation of the efficiency with a specific variable is too small compared to the required uncertainty, this variable should not be considered as part of the calibration, as the uncertainty would hide the effect of such variation. In our case, the variable that produces the lower variation of ε is the density. This variation can reach a relative value of 30%, high enough when compared with the relative uncertainty of the efficiency 5%, justifying then the inclusion of ρ as a variable in the calibration process and, therefore, in the efficiency function.

References

1. Debertin, K., & Helmer, R. G. (1988). *Gamma and X-ray spectrometry with semiconductor detectors*. Amsterdam: Elsevier Science Ltd.
2. Knoll, G. F. (2010). *Radiation detection and measurement* (4th ed.). New York: John Wiley & Sons.
3. Casas-Ruiz, M., Ligero, R. A., & Barbero, L. (2012). Estimation of annual effective dose due to natural and man-made radionuclides in the metropolitan area of the Bay of Cadiz (SW of Spain). *Radiat. Prot. Dosim*., *150*(1), 60–70.
4. Ligero, R. A., Casas-Ruiz, M., Barrera, M., Barbero, L., & Meléndez, M. J. (2010). An alternative radiometric method for calculating the sedimentation rates: Application to an intertidal region (SW of Spain). *Appl. Radiat. Isot*., *68*, 1602–1609.
5. Ligero, R. A., Barrera, M., & Casas-Ruiz, M. (2005). Levels of ^{137}Cs in muddy sediments of the seabed of the Bay of Cádiz, Spain. Part I: Vertical and spatial distribution of activities. *J. Environ. Radioact*., *80*, 75–86.
6. Ligero, R. A., Barrera, M., & Casas-Ruiz, M. (2005). Levels of ^{137}Cs in muddy sediments on the seabed in the Bay of Cádiz, Spain. Part II: Model of vertical migration of ^{137}Cs. *J. Environ. Radioact*., *80*, 87–103.
7. International Organization for Standardization. (1995). *Guide to the expression of uncertainty in measurement*. Geneva, Switzerland: ISO.
8. Bolívar, J. P., García-Tenorio, R., & García-León, M. (1994). A generalized transmission method for gamma-efficiency determination in soil samples. *Nucl. Geophys*., *8*(5), 485–492.
9. Zikovsky, L. (1997). Variation of the detection efficiency of a Ge detector with the height of the sample in Marinelli beaker. *J. Radioanal. Nucl. Chem*., *224*, 171–172.
10. Hubbell, J. H., & Seltzer, S. M. (1995). Tables of x-ray mass attenuation coefficients and mass energy-absorption coefficients 1 keV to 20 MeV for elements

Z = 1 to 92 and 48 additional substances of dosimetric interest. Gaithersburg, MD: National Institute of Standards and Technology (NISTIR 5632). Available from http://physics.nist.gov/xaamdi.

11. Kitto, M. E. (1990). Mass attenuation coefficients of size-fractioned soil. *J. Radioanal. Nucl. Chem.-Lett.*, *145*(3), 175–182.
12. Cutshall, N. H., Larsen, I. L., & Olsen, C. R. (1983). Direct analysis of ^{210}Pb in sediment samples: Self-absorption correction. *Nucl. Instrum. Methods Phys. Res. Sect. B-Beam Interact. Mater. Atoms*, *206*, 309–312.
13. Galloway, R. B. (1991). Correction for sample self-absorption in activity determination by gamma spectrometry. *Nucl. Instrum. Methods Phys. Res. Sect. A-Accel. Spectrom. Dect. Assoc. Equip.*, *300*(2), 367–373.
14. Haase, G., Tait, D., & Wiechen, A. (1993). Monte Carlo simulation of several gamma-emitting source and detector arrangements for determining corrections of self-attenuation and coincidence summation in gamma-spectrometry. *Nucl. Instrum. Methods Phys. Res. Sect. A-Accel. Spectrom. Dect. Assoc. Equip.*, *329*(3), 483–492.
15. Pham, M. K., Sanchez-Cabeza, J. A., Povinec, P. P., Andor, K., Arnold, D., Benmansour, M., Bikit, I., Carvalho, F. P., Dimitrova, K., Edrev, Z. H., Engeler, C., Fouche, F. J., Garcia-Orellana, J., Gasco, C., Gastaud, J., Gudelis, A., Hancock, G., Holm, E., Legarda, F., Ikaheimonen, T. K., Ilchmann, C., Jenkinson, A. V., Kanisch, G., Kis-Benedek, G., Kleinschmidt, R., Koukouliou, V., Kuhar, B., LaRosa, J., Lee, S. -H., LePetit, G., Levy-Palomo, I., Liong Wee Kwong, L., Llaurado, M., Maringer, F. J., Meyer, M., Michalik, B., Michel, H., Nies, H., Nour, S., Oh, J. -S., Oregioni, B., Palomares, J., Pantelic, G., Pfitzner, J., Pilvio, R., Puskeiler, L., Satake, H., Schikowski, J., Vitorovic, G., Woodhead, D., & Wyse, E. (2008). A new Certified Reference Material for radionuclides in Irish Sea sediment (IAEA-385). *Appl. Radiat. Isot.*, *66*(11), 1711–1717.
16. Shakhashiro, A., Gondin da Fonseca Azeredo, A. M., Sansone, U., & Fajgelj, A. (2007). Matrix materials for proficiency testing: optimization of a procedure for spiking soil with gamma-emitting radionuclides. *Anal. Bioanal. Chem.*, *387*(7), 2509–2515.
17. Canberra Industries. (2013). *Model S574 LabSOCS calibration software.* Meriden CT, USA: Canberra Industries Inc. Available from http://www.canberra.com/products/insitu_systems/pdf/ISOCS-SS-C40166.pdf.